



Matrix influence on the OLED emitter Ir(btp)₂(acac) in polymeric host materials – Studies by persistent spectral hole burning

Reinhard Bauer^a, Walter J. Finkenzeller^a, Udo Bogner^a, Mark E. Thompson^b, Hartmut Yersin^{a,*}

^a Universität Regensburg, Institut für Physikalische Chemie, 93040 Regensburg, Germany

^b University of Southern California, Department of Chemistry, Los Angeles, California 90089, USA

ARTICLE INFO

Article history:

Received 28 January 2008

Received in revised form 2 April 2008

Accepted 5 April 2008

Available online 14 April 2008

Keywords:

Triplet emitter

OLED

Persistent spectral hole burning

Zero-field splitting

Polyvinylbutyral

Poly-N-vinylcarbazol

Poly(9,9-dioctylfluoren-2,7-diyl)

Ir(btp)₂(acac)

Phosphorescence line narrowing

Metal-to-ligand charge transfer

PVK

PVB

PFO

MLCT

ZFS

Spin-orbit coupling

SOC

ABSTRACT

Fundamental photophysical properties of the phosphorescent organometallic complex Ir(btp)₂(acac) doped in the polymeric matrices PVK, PFO, and PVB, respectively, are investigated. PVK and PFO are frequently used as host materials in organic light emitting diodes (OLEDs). By application of the laser spectroscopic techniques of phosphorescence line narrowing and persistent spectral hole burning – improved by a synchronous scan technique – we studied the zero-field splitting (ZFS) of the T₁ state into the substates I, II, and III. Thus, we were able to probe the effects of the local environment of the emitter molecules in the different amorphous matrices. The magnitude of ZFS is determined by the extent of spin-orbit coupling (SOC) of the T₁ state to metal-to-ligand charge transfer (MLCT) states. Only by mixings of MLCT singlets, a short-lived and intense emission of the triplet state to the singlet ground state becomes possible. Thus, sufficiently large ZFS is crucial for favorable luminescence properties of emitter complexes for OLED applications. The analysis of the spectral hole structure resulting from burning provides information about the ZFS values and their statistical (inhomogeneous) distribution in the amorphous matrices. For Ir(btp)₂(acac), we found a significant value of ≈18 cm⁻¹ for the splitting between the substates II and III for all three matrices. Interestingly, for PVK the width of the ZFS distribution is found to be ≈14 cm⁻¹ – almost twice as large as for PFO and PVB. Consequently, for a considerable fraction of Ir(btp)₂(acac) molecules in PVK, the ZFS is relatively small and thus, the effective SOC is weak. Therefore, it is indicated that a part of the emitter molecules shows a limited OLED performance.

© 2008 Elsevier B.V. All rights reserved.

1. Introduction

Phosphorescent organo-transition metal complexes are often applied as emitters in organic light emitting diodes (OLEDs) due to their high electroluminescence efficiencies [1]. Ir(btp)₂(acac) ((bis(2,2'-benzothienyl)-pyridinato-N,C^{3'})Iridium(acetylacetonate)), (inset in Fig. 1a) is a well studied OLED emitter [2–10]. It features a saturated red emission peaked at 612 nm [2–4] and a high photolumi-

nescence quantum efficiency. For example, in a film of CBP (4,4'-bis(carbazol-9-yl)biphenyl) a quantum efficiency of ≈50% and an emission decay time of about 6 μs were measured [4,11]. Attractive photophysical properties like these are connected with a significant metal-to-ligand charge transfer (MLCT) character of the emitting T₁ state [12–17]. In particular, the MLCT character promotes quantum mechanical admixtures of higher lying singlet states to the emitting T₁ state via spin-orbit coupling (SOC) [17]. Such admixtures are required to open radiative decay paths from the excited triplet state T₁ to the singlet ground state S₀(0). This means that the photophysical properties important for OLED applications, such as short emission

* Corresponding author.

E-mail address: hartmut.yersin@chemie.uni-regensburg.de (H. Yersin).

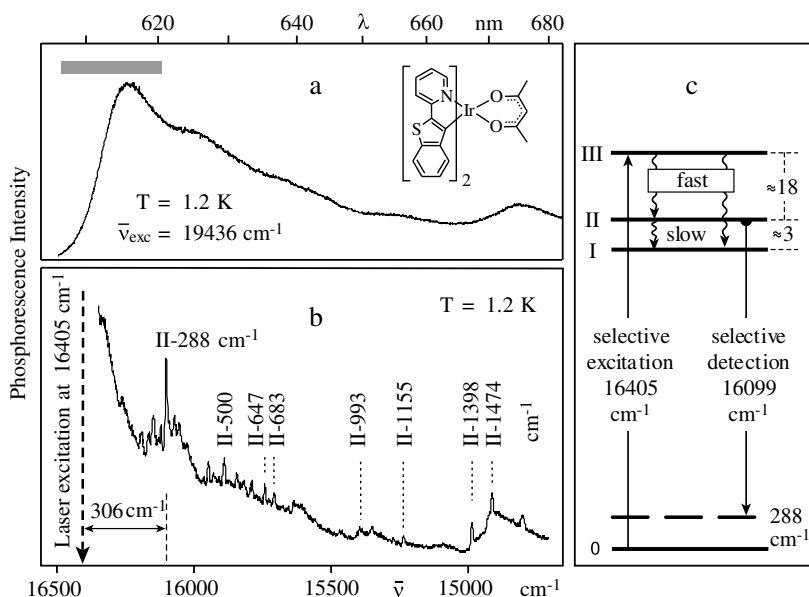


Fig. 1. Emission spectra of Ir(btp)₂(acac) in PFO upon excitation at (a) 19,436 cm⁻¹ and at (b) 16,405 cm⁻¹. Phosphorescence line narrowing can be obtained by excitation in the region between about 16,100 cm⁻¹ and 16,500 cm⁻¹ (shaded bar in (a)). The intensity of the vibrational zero-phonon line (ZPL) at a spectral distance of 306 cm⁻¹ from the exciting laser energy was used for probing of the spectral holes (see Fig. 2). Both spectra were measured in superfluid Helium at 1.2 K. The inset in (a) shows the chemical structure of Ir(btp)₂(acac). (c) Reproduces the energy level diagram for the triplet substates and depicts selected radiative and radiationless deactivation paths. The dashed line represents the vibrational level of the 288 cm⁻¹ ground state mode.

decay times and high photoluminescence quantum yields, are governed by the extent of MLCT character in the emitting triplet term [12–17]. As the MLCT character is correlated to the magnitude of zero-field splitting (ZFS) of the T₁ state into substates I, II and III (compare e.g. Refs. [12–17]) and as the individual features of these substates are responsible for the emission properties, it is of high interest to investigate the characteristics of the substates in more detail. Very recently, it has been shown that the photophysical properties of the triplet state of Ir(btp)₂(acac) distinctly depend on the environment of the emitter complex. Emission decay times, ZFSs, spin-lattice relaxation times [18], etc., are different for different sites of the Ir complex in the matrix [12–14]. For example, the energy separations between the three T₁ substates of Ir(btp)₂(acac) have been determined on the basis of highly resolved spectra in polycrystalline hosts, such as octane or dichloromethane [12,13]. Hereby, it was found that the magnitude of ΔE(ZFS) can differ by almost a factor of two for different sites in the same host material [12]. Therefore, the influence of the host, especially of OLED relevant hosts, on the ZFS (and thus on essential photophysical properties) is of high interest.

However, with amorphous hosts – as typically used for emission layers in OLEDs – only very broad emission bands are observed. In this situation, indirect approaches of analyzing the temperature dependence of emission decay data were used to provide information about the individual properties of the triplet substates (for example, see Refs. [14,17]). On the other hand, luminescence line narrowing [19] and persistent spectral hole burning [20] represent methods which allow for high-resolution

spectroscopy of dye molecules doped into amorphous hosts.¹ Most of the work published to date concerns singlet-singlet transitions (e.g. see Refs. [20–22]), but also singlet-triplet transitions [23–25] and transitions between levels of higher multiplicity [26–28] have been investigated. However, these methods have not yet been applied to OLED relevant emitter/matrix systems.

In the present study, we report on persistent spectral hole burning as a method for the investigation of the ZFS and its inhomogeneous distribution applied to the emitting triplet state of Ir(btp)₂(acac) doped into a common polymer (PVB = polyvinylbutyral) and two polymers which are frequently applied in OLEDs (PVK = poly-N-vinylcarbazol, PFO = (poly(9,9-dioctylfluoren-2,7-diyl)). One goal is to obtain information on how the ZFS data obtained in Shpol'skii and Shpol'skii-like matrices relate to the properties of emitter complexes in an amorphous matrix. Further, we are interested in the inhomogeneous distribution of the ZFS values and thus of the MLCT character of the emitting triplet states. An analysis provides information about photophysical differences of the various subsets of molecules in the same amorphous matrix. The discussion indicates that a fraction of the molecules in polymer OLED matrices can exhibit less favorable emission properties for OLED applications.

2. Experimental

The samples of PVB (polyvinylbutyral, Hoechst), PVK (poly-N-vinylcarbazol, Acros) and PFO (poly(9,9-dioctylflu-

¹ The corresponding methods are explained in Sections 3.1 and 3.3, respectively.

oren-2,7-diyl), Aldrich) doped with Ir(btp)₂(acac) at concentrations of about 10⁻³ mol/l were prepared as films of about 100 μm thickness from solution, using ethanol (PVB) or dichloromethane (PVK, PFO) as solvents. The complex was synthesized according to the procedure described in Ref. [2]. Spectral holes were burnt and probed with a (Spectra-Physics Model 380) dye ring laser with a spectral band width of about 0.1 cm⁻¹. The laser wavelength was scanned by turning the birefringent filter by means of a DC motor and recorded by a wavemeter (Burleigh WA20-VIS). For non-selective excitation, the 514.5 nm line of the Ar ion pump laser was used. The samples were immersed in an optical Helium bath cryostat which could be cooled down to $T = 1.2$ K by pumping off the He vapor. The emitted phosphorescence light was dispersed by a Spex 1401 double monochromator and detected by photon counting with a cooled RCA C7164R photomultiplier.

3. Results and discussion

3.1. Phosphorescence line narrowing for Ir(btp)₂(acac) in the amorphous PFO host

The emission spectrum of Ir(btp)₂(acac) doped into PFO strongly depends on the excitation energy. When a narrow-line excitation is chosen at a high energy, for example at 19,436 cm⁻¹ (514.5 nm), which lies in the region of the homogeneously broadened $S_0 \rightarrow {}^1\text{MLCT}/{}^3\text{MLCT}$ transitions [12], the usual and well-known broad-band emission spectrum is obtained, even at $T = 1.2$ K (Fig. 1a). However, upon narrow-line excitation within the inhomogeneously broadened $S_0 \rightarrow T_1$ transition range between about 16,100 and 16,500 cm⁻¹ (shaded bar in Fig. 1a), for example at 16,405 cm⁻¹, a well-resolved emission spectrum can be recorded, even in this amorphous polymer host (Fig. 1b). In this case, the laser excites dominantly just that specific site of Ir(btp)₂(acac) in PFO, which has an electronic 0–0 transition precisely at the chosen excitation energy. More exactly, due to the zero-field splitting of the T_1 term into the substates **I**, **II**, and **III** and due to the much higher transition probability of the transition $0 \rightarrow \text{III}$ compared to $0 \rightarrow \text{II}$, $0 \rightarrow \text{I}$, specifically those molecules will be excited with preference, which have their $0 \rightarrow \text{III}$ transition at the laser energy. (The $0 \rightarrow \text{III}$ transition probability is by one and two orders of magnitude larger than that of the transition $0 \rightarrow \text{II}$ and $0 \rightarrow \text{I}$, respectively [12,13]). The structure displayed in Fig. 1b represents part of a resolved vibrational satellite structure [14] which stems from a triplet substate. Although substate **III** is excited selectively, emission from this state is not observed at low temperature. This is due to fast relaxation, i.e. fast spin-lattice relaxation (SLR), from this state to the two lower lying substates [13,14,18] (Fig. 1c). On the other hand, SLR between the substates **II** and **I** is very slow [13]. Thus, these two triplet substates both emit, even at $T = 1.2$ K. Analysis of the vibrational satellite structure of Ir(btp)₂(acac) doped into a crystalline CH₂Cl₂ matrix, as carried out in Ref. [14], allows us to identify most of the satellites in the line-narrowed spectrum shown in Fig. 1b. The dominant line represents a vibrational satellite stemming from substate **II** and is induced by a 288 cm⁻¹ Franck-Condon active mode (Fig. 1c) [14].

This line is found 306 cm⁻¹ below the excitation energy. This value fits well, if it is assumed that substate **III** lies 18 cm⁻¹ above substate **II** (288 cm⁻¹ + 18 cm⁻¹ = 306 cm⁻¹). The value of 18 cm⁻¹ lies within the range of $\Delta E(\text{ZFS})$ energies as determined in Ref. [12]. An independent confirmation of this splitting energy is given below. The 288 cm⁻¹ vibrational satellite line – a so-called vibrational zero-phonon line (ZPL) – is accompanied by a phonon sideband at the low-energy side. This band results from couplings of low-energy vibrational modes of the complex in its matrix cage to the electronic structure/transition. These modes, often called local phonon modes (resulting from hindered rotational motions of the emitter molecules in their matrix cages), have energies in the range of 15–30 cm⁻¹. They frequently occur together with purely electronic 0–0 transitions and also – as shown in Fig. 1b – together with vibrational ZPLs [14,15].

As characteristic of phosphorescence line narrowing, the spectral shift between the exciting laser energy and the specific vibrational satellite line is almost independent of the excitation energy, when it lies within the inhomogeneously broadened absorption band. The absorption in the region of the electronic 0–0 transition depends on the excitation energy due to a varying spectral density of resonantly absorbing molecules.

For the investigations presented in this study, the vibrational satellite with a shift of 306 cm⁻¹ relative to the exciting laser is selected for the detection of the spectral holes by a specific synchronous scanning method. This method will be described in the next section.

The specific vibrational satellite $0 \rightarrow 0 + 288$ cm⁻¹ (representing a vibrational zero-phonon line) can be observed in the phosphorescence line-narrowed spectra of the Ir(btp)₂(acac) complex for all three matrices. The width of this line is ≈ 7 cm⁻¹ in PFO and PVB, while it is ≈ 18 cm⁻¹ in PVK. The 288 cm⁻¹ vibrational ZPL in the PFO matrix has the highest intensity relative to the background compared to the other matrices.

3.2. Detection of spectral holes by a synchronous excitation-detection scan technique

The intensity of a vibrational satellite (vibrational ZPL) depends linearly on the number of resonantly absorbing emitter molecules. Thus, the spectral dependence gives information about the inhomogeneous distribution. Using this relation, persistent spectral holes – after having been burnt (Section 3.3) – are probed in a luminescence excitation technique as schematically depicted in Fig. 2. Hereby, a narrow-line light source of relatively weak intensity excites a subset of molecules within the range of the inhomogeneously broadened band of the purely electronic transition. The detection energy is set to the maximum of a specific (resolved) vibrational satellite. Now scanning the excitation energy, while keeping the energy difference between detection and excitation constant, reproduces the inhomogeneous distribution function. If a persistent spectral hole has been burnt into this distribution (Section 3.3), the reduced density of resonantly absorbing molecules at the burning energy is directly displayed in the excitation spectrum (dashed structure in Fig. 2).

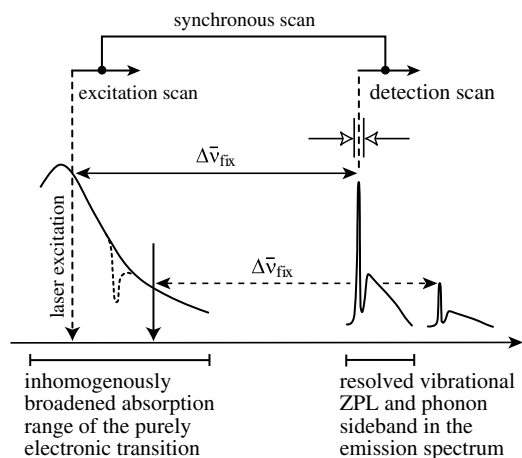


Fig. 2. Schematic diagram to illustrate the synchronous scan technique for the measurement of luminescence excitation spectra. The tunable narrow-line laser light (vertical arrow) excites preferentially a strongly absorbing subset of emitter molecules within its inhomogeneously broadened, purely electronic absorption range. At low temperature, a spectrum results, which usually consists of several vibrational zero-phonon satellite lines (ZPL, vibrational satellites) and the corresponding phonon sidebands, as explained in Section 3.1. In this diagram, only one ZPL with its phonon sideband is displayed. The inhomogeneous distribution of the purely electronic transitions is obtained by tuning the detection wavelength synchronously with a fixed energy separation $\bar{\nu}_{\text{fix}}$ relative to the excitation energy. For detection, a vibrational ZPL is chosen, which occurs with high intensity. The amplitude of the signal in emission is almost proportional to the number of resonantly excited molecules. The dashed spectral structure shows the modified band after burning of a persistent spectral hole (see Section 3.3).

For the experiments described in this investigation, the vibrational ZPL with a shift of 306 cm^{-1} was used (see Section 3.1, Fig. 1b) primarily because of the high intensity of this satellite relative to the background intensity. According to the discussion presented in Section 3.1, the resonant absorption of T_1 substate III is by far the strongest among the three triplet substates of $\text{Ir}(\text{btp})_2(\text{acac})$ [12–14]. Therefore, we infer that this synchronous scanning technique maps dominantly the inhomogeneous distribution function (absorption) of the $\text{O} \rightarrow \text{III}$ transition, as long as no vibrational levels of lower lying emitters (e.g. $\text{O} \rightarrow \text{III} + \bar{\nu}_0$) are involved in the excitation process. In order to avoid complications due to the excitation of such vibrational levels, we performed the hole burning experiments at the long-wavelength side of the inhomogeneous distribution. This is the first time that this synchronous scan technique has been reported.

3.3. Persistent spectral hole burning of triplet substates in different amorphous hosts

Narrow-line and intense excitation within an inhomogeneously broadened electronic transition of a light absorbing species leads to reduced absorption of the sample at the excitation (laser) energy in the course of the laser excitation, and thus to the burning of a persistent spectral hole in the absorption or luminescence excitation spectrum [20]. The persistent spectral hole is a consequence of a photophysical or a photochemical burning mechanism.

In addition to the spectral holes (reduced absorptions), areas of weakly increased absorption (anti-holes) are also formed. If the anti-holes lie close to the burning energy, in the spectral range of the inhomogeneously broadened electronic transition, a photophysical hole burning mechanism is indicated. This mechanism can be explained by phonon-induced barrier crossings within asymmetric double well potentials² which are characteristic for disordered systems [29]. Such a barrier crossing corresponds, for example, to a rearrangement of the light absorbing species in its matrix cage or of any other atom, ion or molecule in the immediate neighborhood (compare e.g. Ref. [30]). During the hole burning process, the transfer from one potential minimum to another one results in a different absorption energy of the light absorbing species. At low temperature, this new situation can be stable and a persistent spectral hole results. Persistent photophysical hole burning can occur in amorphous materials or in systems with at least local disorder [21,29–31]. Photochemical hole burning, on the other hand, is usually related to anti-holes which occur in more distant energy regions relative to the burning (laser) energy, since in this case the molecular structure is changed.

Persistent spectral holes can provide spectral structures in the absorption range of the purely electronic transition, which are several orders of magnitude narrower than the inhomogeneously broadened band. As a consequence, high-resolution spectroscopy is possible, if the absorption can be scanned over the range of the burnt hole. Since the existence of zero-phonon lines is required, most hole burning experiments are carried out at liquid He temperatures.

With $\text{Ir}(\text{btp})_2(\text{acac})$ doped into the amorphous PVB host, we observed persistent spectral hole burning at $T = 1.2\text{ K}$ (Fig. 3). At a short burning time, e.g. of $t_b = 130\text{ s}$, a spectral hole can be seen only at the energy of the burning laser (hole A in Fig. 3a). With increasing burning time, the spectrum changes. Successively, an additional narrow hole component develops at the high-energy side and a broad hole appears at the low-energy side of the laser energy. The left part of Fig. 3 shows the spectral hole structure in PVB after three different burning times t_b with a burning intensity of about 10 W/cm^2 at $16,500\text{ cm}^{-1}$. The width (FWHM) of the resonant hole A increases from 1.7 cm^{-1} after 130 s to 2.4 cm^{-1} after 2480 s. Since we observed that the width of the resonant hole depends only on the duration of the hole burning and not on the power density of the burning laser, local heating is not expected to be responsible for the increase of the width. This increase rather is attributed to dynamical processes in the double well potentials in the course of the burning, which lead to slight spectral line shifts and as a consequence to a line broadening. The side hole shifted by about 18 cm^{-1} from the resonant hole to the high-energy side has a width of 6.4 cm^{-1} . The relatively broad asymmetric hole which

² A more precise description requires the knowledge of the potential hypersurface. However, for the treatment of a hole burning process by a phonon induced crossing of a barrier between two minima of the potential hypersurface, it is usually sufficient to replace this hypersurface by asymmetric double well potentials. Thereby, only the knowledge of the asymmetry and the barrier height are necessary [29].

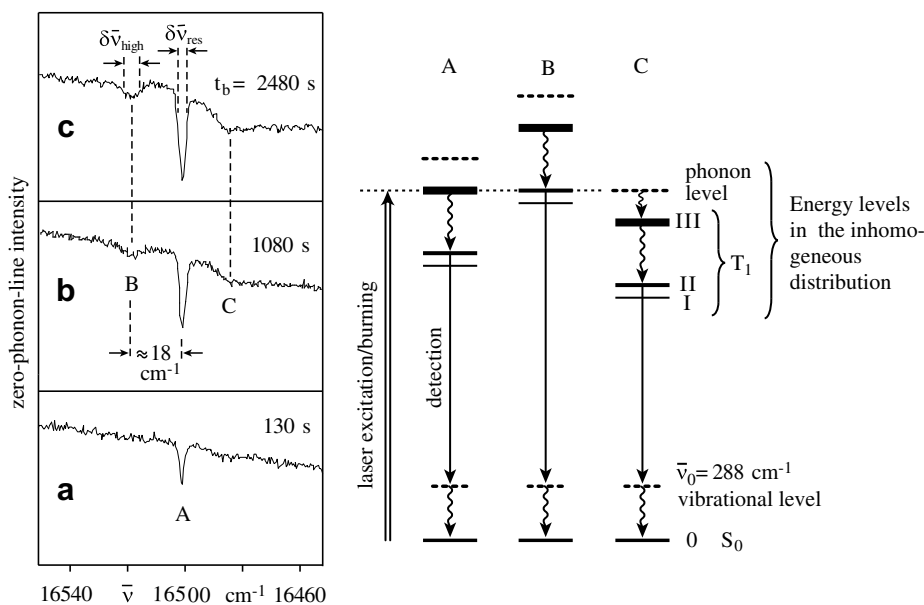


Fig. 3. Persistent spectral holes burnt at $16,500\text{ cm}^{-1}$ in the guest/host system $\text{Ir}(\text{btp})_2(\text{acac})/\text{PVB}$ after different burning times t_b at $T = 1.2\text{ K}$. The spectral holes were probed by recording the intensity of the strong vibrational satellite (vibrational ZPL) shifted by 306 cm^{-1} relative to the exciting laser energy. The emission stems from substate **II** and is detected at the 288 cm^{-1} vibrational satellite. The diagram on the right hand side displays energy level schemes of three different subsets A, B, and C of molecules which lie within the inhomogeneous distribution. At a fixed laser energy, the laser burns at different levels with different absorption strengths of the doped molecules. Thus, three hole components A, B, and C result. The differences of the absorption cross sections are indicated by the thicknesses of the levels representing the triplet substates **I**, **II**, and **III**, respectively, and the dashed lines above substate **III** represent a phonon level of this substate. From the different hole components A and B and their evolution with burning time, the relative absorption cross sections of the transitions to the T_1 substates **II** and **III**, the amount of energy splitting and, in particular, the distribution of these splittings can be determined. $\delta\bar{\nu}_{\text{res}}$ and $\delta\bar{\nu}_{\text{high}}$ represent the half widths (FWHM) of the resonant hole and of the high-energy side hole, respectively.

appears at the low-energy side is shifted by about 17 cm^{-1} . While the central component is almost saturated after 1080 s, the side components still deepen with further burning time. Quantitative analysis by fitting with Gaussian line shapes indicates that the central hole component has about the same area after 130 s burning time as the high-energy component after 1080 s (for a quantitative explanation see below).

After sufficient burning time, the measured hole spectrum shows a triple structure, with the central hole resonant with the burning laser energy, and two side holes – one low-energy and one high-energy component. Taking into account that probing displays the inhomogeneous distribution of the T_1 substate **III** (see Section 3.1), it can be concluded that with increasing burning time different subsets of emitter molecules are involved. Burning is most efficient for molecules with highest absorption cross section, i.e. for those molecules with the energy of their substate **III** at the laser energy. Thus, the central component can be attributed to burning of molecules absorbing the laser by their $0 \rightarrow \text{III}$ transition (compare subset “A” in Fig. 3).

$\text{Ir}(\text{btp})_2(\text{acac})$ complexes with their T_1 substate **II** in resonance with the burning laser have their substate **III** blue shifted by the corresponding ZFS value of $\Delta E_{\text{III,II}}$. Therefore, the high-energy hole component can be attributed to the burning of $\text{Ir}(\text{btp})_2(\text{acac})$ complexes which absorb at the laser energy with their $0 \rightarrow \text{II}$ transition (compare subset “B” in Fig. 3). The measured energy difference of both hole

components represents the energy difference $\Delta E_{\text{III,II}}$. A value of about 18 cm^{-1} is found. A similar value of ZFS is reported in Refs. [12–14]. In these studies, highly resolved spectra of $\text{Ir}(\text{btp})_2(\text{acac})$ doped into polycrystalline dichloromethane and octane, respectively, were investigated.

The hole component shifted by 17 cm^{-1} to the red originates from molecules, which are burnt by absorption of energy levels above the T_1 substate **III**. The most probable explanation is an absorption (burning) into a localized phonon of the excited substate **III** (compare subset C in Fig. 3), since spectral shape and energy of this low-energy side hole resemble those of typical phonon side bands [15].

From the longer build-up time of the high-energy hole component relative to the central component the ratio of absorption cross sections for the transitions to the involved triplet substates **II** and **III** can be estimated. The hole area of the central component in PVB after 130 s burning time is in good approximation the same as the area of the blue shifted component after 1080 s. Assuming the same hole burning quantum yields for both subsets of molecules, the difference of burning times can be attributed to the different absorption cross sections. Accordingly, the absorption cross section of the transition from the singlet ground state S_0 to substate **III** can be estimated to be by a factor of ≈ 8 higher than that of the transition to substate **II**. This value lies in the range found for the ratios of emission decay times from the studies of different sites of $\text{Ir}(\text{btp})_2(\text{acac})$ in CH_2Cl_2 [13].

The absorption cross section of the $0 \rightarrow I$ transition of $\text{Ir}(\text{btp})_2(\text{acac})$ is several times lower than those of the transitions to the substates **II** and **III**. Therefore, the observation of the corresponding side holes would require substantially longer burning times, which was not feasible with the available experimental equipment. Consequently, substate **I** is not displayed in the hole burning spectra.

For completeness, it is remarked that anti-hole areas were observed within the inhomogeneous distribution of the electronic transitions of the emitter molecules in the matrix. For example, an anti-hole is manifested in the small intensity increase in the spectral range between hole A and hole B (in Fig. 3 curve for $t_b = 2480$ s). This intensity increase (representing an increase of the absorption) is enhanced with further burning, i.e. the anti-hole becomes more distinct. The occurrence of anti-holes in this spectral range indicates a photophysical hole burning mechanism.

Spectral hole burning was also observed with $\text{Ir}(\text{btp})_2(\text{acac})$ embedded in PFO and PVK, respectively. Fig. 4 compares hole spectra for the three matrices, whereby the spectrum depicted in Fig. 4a is the same as the one shown in Fig. 3 after 2480 s burning time. The hole in PFO was burnt with an intensity of about 100 W/cm^2 for 10 min resulting in a width of 2.6 cm^{-1} of the resonant component (Fig. 4b). Here, the high-energy component is also shifted by about 18 cm^{-1} and has a width of about 8 cm^{-1} . The separation of the hole components is practically identical to the one found for $\text{Ir}(\text{btp})_2(\text{acac})$ doped into PVB. The low-energy component, however, has its minimum shifted by about 15 cm^{-1} and is the least pronounced one in all matrices investigated. The latter observation is in accordance with a comparatively weak electron–phonon coupling in PFO.

In the PVK matrix, $\text{Ir}(\text{btp})_2(\text{acac})$ showed significantly lower burning efficiency than in PFO (Fig. 4c). After 4200 s of burning with a strongly focused laser beam of about 1000 W/cm^2 , the resulting central hole exhibits a width of about 4.5 cm^{-1} . This implies that a factor of about 170 more photons were used per unit area to burn the hole

in PVK compared to PFO (Fig. 4). This behavior can be attributed to differences of the double well potentials in the different hosts. A more detailed explanation requires further studies.

Concerning the side holes, the spectra of the holes for the PVK matrix differ from those of the other two matrices examined here. For the high-energy hole, the blue shift of the minimum is estimated to be $\approx 18 \text{ cm}^{-1}$ relative to the central component, but its width of $\approx 15 \text{ cm}^{-1}$, as determined by a fit of a Gaussian line shape, is roughly twice as large as in PFO or PVB. Local heating during burning cannot be responsible for this larger width as it is also observed with a less intense burning laser. The low-energy contribution has its minimum at $\approx 14 \text{ cm}^{-1}$ red shifted relative to the central component, which is similar to the corresponding shift in PFO.

Interestingly, the half widths of the high-energy hole components – determined in good approximation as FWHM widths of Gaussian hole shapes – reveal that the ZFS values between the T_1 substates **II** and **III** are distributed over significant ranges. For an estimation of the corresponding distributions, a convolution of Gaussian distributions and line shapes is assumed. Then, the half width (FWHM) of the distribution of the ZFS between substates **II** and **III** $\delta(\Delta E_{\text{II,III}})$ can be obtained from the half widths (FWHM) of the high-energy hole $\delta\bar{\nu}_{\text{high}}$ and of the corresponding resonant hole $\delta\bar{\nu}_{\text{res}}$ according to [32]

$$(\delta(\Delta E_{\text{II,III}}))^2 = (\delta\bar{\nu}_{\text{high}})^2 - (\delta\bar{\nu}_{\text{res}})^2. \quad (1)$$

Thus, we find values for $\delta(\Delta E_{\text{II,III}})$ of approximately 6 cm^{-1} and 7 cm^{-1} for PVB and PFO, respectively, and of $\approx 14 \text{ cm}^{-1}$ for PVK. This demonstrates that the inhomogeneous distribution of the ZFS values $\Delta E_{\text{II,III}}$ is significantly broader for PVK than for the other two hosts. Obviously, $\text{Ir}(\text{btp})_2(\text{acac})$ exhibits a more pronounced interaction with PVK than with the other two matrices. Possibly, this is due to π -interactions of the (btp) ligand of the Ir complex with the carbazole ring system of PVK. A corresponding interaction is not present in PVB and would also be absent in PFO, if $\text{Ir}(\text{btp})_2(\text{acac})$ is hosted near the alkyl chains.

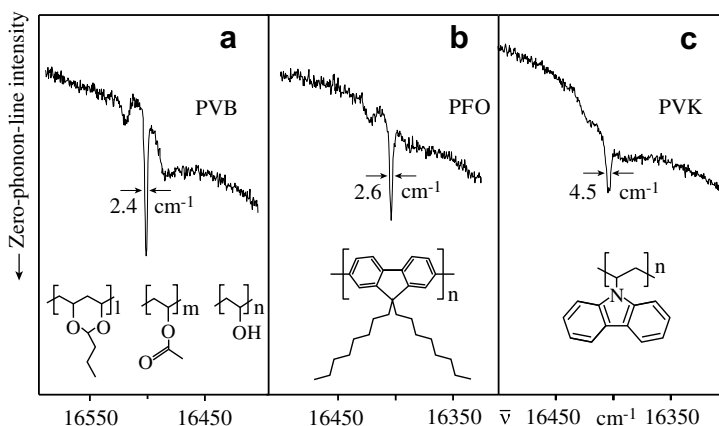


Fig. 4. Persistent spectral holes of $\text{Ir}(\text{btp})_2(\text{acac})$ in three amorphous polymeric matrices (a) PVB, (b) PFO, and (c) PVK at $T = 1.2 \text{ K}$. The holes, burnt at $16,400 \text{ cm}^{-1}$ (PVK and PFO) and $16,500 \text{ cm}^{-1}$ (PVB), were probed by recording the intensity of an emission peak which lies 306 cm^{-1} below the energy of the probing laser. The insets show the chemical structures of the polymers. PVK and PFO are homopolymers, while PVB is built-up by three constitutional units, which are statistically distributed along the polymer chain with $l > n > m$.

The low-energy hole component is shallowest among the three investigated matrices in PFO. This is in accordance with a comparatively weak electron–phonon coupling in this matrix, which is supported by the observation that the line-narrowed spectra of Ir(btp)₂(acac) in PFO show well resolvable vibrational satellite lines (Section 3.1). This result is important for future investigations of other organo-transition metal complexes, if highly resolved spectra are desired.

4. Assignments and conclusion

The present study shows that persistent spectral hole burning and phosphorescence line narrowing provide powerful tools to gain insight into the splitting structure of the emitting triplet state **T**₁ of Ir(btp)₂(acac) into substates, even when the compound is doped into amorphous matrices, which are frequently applied in OLEDs. The obtained results are in line with the findings of previous investigations in Shpol'skii and Shpol'skii-like hosts [12]. In these studies, ZFS values were determined for different discrete sites of Ir(btp)₂(acac) in CH₂Cl₂. $\Delta E_{\text{III,II}}$ values were found to lie between 12 and 24 cm⁻¹. In the present investigation, mean values of 18 cm⁻¹ have been found for the splitting between the substates **II** and **III**. With the method of spectral hole burning, it was not possible to assess the weakly absorbing substate **I**. However, the separation between substate **I** and the next higher lying substate **II** is assumed to be also about 3 cm⁻¹, as found for Shpol'skii-like matrices [12]. In this case the (mean) total ZFS can be estimated to about 21 cm⁻¹ for all three matrices. Indeed, these values lie well within the range found in the polycrystalline Shpol'skii matrices. Prior to our work, this detailed information has not been obtained for triplet emitters embedded in *amorphous* hosts.

The amount of $\Delta E(\text{ZFS})$ is correlated with the extent of MLCT character in the emitting triplet term mixed in mainly via spin–orbit coupling [17]. Thus, a variation of $\Delta E(\text{ZFS})$ in dependence of the compounds' environment (host cage) indicates a change of the interaction of host molecules with the electronic states of the dopant. Such a behavior is not unusual, since the host cage can alter the geometry of the dopant, cause changes of the ligand field strength, induce π – π interactions between host and guest, etc. As consequence, shifts of ^{1,3} $\pi\pi^*$ and/or ^{1,3}MLCT states can occur. Due to such changes, state mixings will be altered and can lead to differently effective SOC. Thus, for example, smaller singlet admixtures to the emitting triplet state and also a smaller $\Delta E(\text{ZFS})$ can result. Among the different matrices studied, PVK induces the strongest inhomogeneous spread of the splitting between the substates **II** and **III** ($\Delta E_{\text{III,II}}$). As a consequence, a substantial fraction of the Ir(btp)₂(acac) complexes doped into PVK have only small splittings around 10 cm⁻¹. Such values might already be too small to enable luminescence properties as required for OLED applications. This is indicated, since for emitter compounds with small ZFS values, spin–orbit coupling is relatively weak and thus, the important mixing of singlet character into the triplet substates is not effective. Therefore, such complexes exhibit compar-

tively small radiative decay rates and often also small quantum yields [12–14].

It should be remarked that efficient OLED triplet emitters hitherto studied exhibit significant or even large zero-field splittings of the **T**₁ parent term. In this context, a value of ≈ 10 cm⁻¹ may already be considered as critical.

We suppose that the results obtained for the compound in amorphous matrices at low temperature hold also at ambient temperature, if the matrices are considered to be rigid enough. This seems to be valid for host materials with a glass transition temperature T_g being significantly larger than 300 K.

In future investigations, we will use persistent spectral hole burning as a sensitive probing technique for the effects of external electric fields [31] on optical transitions in OLED emitter materials. We expect that the analysis of electric field induced shifts of the electronic levels will provide more detailed information on the interaction of the emitter complex with its closest environment, particularly, with regard to the fact that emitters in OLEDs are exposed to high electric fields.

Acknowledgements

We thank the *Bundesministerium für Bildung und Forschung (BMBF)* for providing the funding of this investigation. The *BaCaTeC* is acknowledged for financial support of the exchange with the University of Southern California.

References

- [1] H. Yersin (Ed.), *Highly Efficient OLEDs with Phosphorescent Materials*, Wiley-VCH, Weinheim, 2008.
- [2] S. Lamanski, P. Djurovich, D. Murphy, F. Abdel-Razzaq, H.-E. Lee, C. Adachi, P.E. Burrows, S.R. Forrest, M.E. Thompson, *J. Am. Chem. Soc.* 123 (2001) 4304.
- [3] F.-C. Chen, Y. Yang, M.E. Thompson, J. Kido, *Appl. Phys. Lett.* 80 (2003) 2308.
- [4] C. Adachi, M.A. Baldo, S.R. Forrest, S. Lamanski, M.E. Thompson, R.C. Kwong, *Appl. Phys. Lett.* 78 (2001) 1622.
- [5] S. Lamanski, P. Djurovich, F. Abdel-Razzaq, S. Garon, D. Murphy, M.E. Thompson, *J. Appl. Phys.* 92 (2002) 1570.
- [6] S. Tokito, M. Suzuki, F. Sato, M. Kamachi, S. Shirane, *Org. Electr.* 4 (2003) 105.
- [7] X. Chen, J.-L. Liao, Y. Liang, M.O. Ahmed, H.-E. Tseng, S.-A. Chen, *J. Am. Chem. Soc.* 125 (2003) 636.
- [8] S. Tokito, T. Iijima, T. Suzuki, F. Sato, *Appl. Phys. Lett.* 83 (2003) 2459.
- [9] F.-C. Chen, Y. Yang, Q. Pei, *Appl. Phys. Lett.* 81 (2002) 4278.
- [10] T. Echigo, S. Naka, H. Okada, H. Onnagawa, *Jpn. J. Appl. Phys.* 44 (2005) 626.
- [11] Y. Kawamura, K. Goushi, J. Brooks, J.J. Brown, H. Sasabe, C. Adachi, *Appl. Phys. Lett.* 86 (2005) 071104.
- [12] W.J. Finkenzeller, T. Hofbeck, M.E. Thompson, H. Yersin, *Inorg. Chem.* 46 (2007) 5076.
- [13] W.J. Finkenzeller, M.E. Thompson, H. Yersin, *Chem. Phys. Lett.* 444 (2007) 273.
- [14] H. Yersin, W.J. Finkenzeller, in: H. Yersin (Ed.), *Highly Efficient OLEDs with Phosphorescent Materials*, Wiley-VCH, Weinheim, 2008, p. 1.
- [15] H. Yersin, D. Dinges, *Top. Curr. Chem.* 214 (2001) 82.
- [16] H. Yersin, *Top. Curr. Chem.* 241 (2004) 1.
- [17] A.F. Rausch, H.H.H. Homeier, P.I. Djurovich, M.E. Thompson, H. Yersin, in: Z. Kafafi, F. So (Eds.), *Proceedings of SPIE Optics and Photonics – Organic Light Emitting Materials and Devices XI*, San Diego 2007, vol. 6655, p. 66550F.
- [18] H. Yersin, J. Strasser, *Coord. Chem. Rev.* 208 (2000) 331.
- [19] R.I. Personov, in: V.R. Agranovich, R.M. Hochstrasser (Eds.), *Spectroscopy and Excitation Dynamics of Condensed Molecular Systems*, North Holland, Amsterdam, 1983, p. 555.

- [20] W.E. Moerner (Ed.), *Persistent Spectral Hole-burning: Science and Applications*, Springer, Berlin, 1988.
- [21] U. Bogner, R. Schwarz, *Phys. Rev. B* 24 (1981) 2846.
- [22] T. Attenberger, U. Bogner, M. Maier, *Chem. Phys. Lett.* 180 (1991) 207.
- [23] S. Lin, J. Fünfschilling, I. Zschokke-Gränacher, *J. Lumin.* 40 (1988) 513.
- [24] H. Riesen, E. Krausz, *Chem. Phys. Lett.* 182 (1991) 266.
- [25] H. Riesen, E. Krausz, L. Wallace, *J. Phys. Chem.* 96 (1992) 3621.
- [26] B. Kozankiewicz, J. Bernard, E. Migirdicyan, M. Orrit, M.S. Platz, *Chem. Phys. Lett.* 245 (1995) 549.
- [27] B. Kozankiewicz, A.D. Gudmundsdottir, M. Orrit, M.S. Platz, Ph. Tamarat, *J. Lumin.* 86 (2000) 261.
- [28] H. Riesen, *Coord. Chem. Rev.* 250 (2006) 1737.
- [29] U. Bogner, *Phys. Rev. Lett.* 37 (1976) 909.
- [30] K.M. Murdoch, T. Attenberger, U. Bogner, G.D. Jones, *J. Phys. Chem. Solids* 58 (1997) 1513.
- [31] U. Bogner, in: G. Mahler, V. May, M. Schreiber (Eds.), *Molecular Electronics: Properties Dynamics and Applications*, Marcel Dekker, New York, 1996, p. 233.
- [32] H. Cramér, *Mathematische Zeitschrift* 41 (1936) 405.